Raman scattering of light in a degenerate (Pb, Sn) Se semiconductor

L. K. Vodop'yanov
P. N. Lebedev Physics Institute, Academy of Sciences of the USSR, 117924, Moscow

L. A. Fal'kovskiĭ
L. D. Landau Institute of Theoretical Physics, Academy of Sciences of the USSR, 117334, Moscow

J. Irvin and S. Himenis
Simon Freser University, Barnaby, Canada

(Submitted 22 April 1991)
Pis'ma Zh. Eksp. Teor. Fiz. **53**, No. 11, 561–565 (10 June 1991)

The broad peak in the spectrum is interpreted as the electronic component of the Raman scattering.

Quasi-binary compounds $Pb_{1-x}Sn_xSe$ attract attention because of their unusual physical properties. A change in their composition and temperature causes a band inversion which changes the width of the band gap from 0.3 eV to zero. In addition, these compounds have a large dielectric constant, high mobility, and a small effective mass of the charge carriers. The phonon spectrum of (Pb, Sn)Se alloys was initially studied in Refs. 1 and 2 using neutrons, and these spectra were calculated in Ref. 3. Neutron methods of investigation are complex and require the use of large, high-quality crystals.

In the present letter we report the results of the first experimental studies of Raman scattering of light in semiconductor compounds $Pb_{1-x}Sn_xSe$ ($x = 0.07$–0.42). The large concentration of carriers, the opacity of the testy crystals to the exciting laser light and the small effective scattering cross section complicate Raman spectroscopy considerably. To obtain reliable experimental results, we used a laboratory model of a computer-controlled Raman spectrometer, in which the weak scattered light was detected by means of an optical multichannel analyzer with an ITT F4146 "Mepsicron" signal storage device. The total spectrum was recorded simultaneously by 10^3 channels of a microchannel plate with a position-sensitive resistive anode. Such a system is characterized by an extremely low dark current amounting to approximately 0.05 counts/s. For the given signal-to-noise ratio the recording efficiency increases by a factor of 10^3 in comparison with the standard one-channel arrangement. To suppress the scattered light near the exciting line, we built a triple monochromator with halographic diffraction gratings which were connected in a "dispersion-subtraction arrangement." The use of a monochromator reduced the light scattering intensity by 4–5 orders of magnitude.

The Raman spectra were measured in an inverse-scattering geometry. To prevent an overheating of the sample, we installed a cylindrical lens in the laser-beam channel. The measurements were carried out in a vacuum and the sample was placed at the cold stage of the helium cryostat with a regulated temperature. The surface of the

samples was polished mechanically with a diamond powder and then etched electrolytically.

The first measurements of the Raman spectra did not give positive results: the signal appeared at the noise level. To increase the intensity of the signal, we made use of the resonance intensification, where the energy of the exciting light is close to the energy of one of the electronic transitions. At the point L in the calculated band diagram[4] the frequency of one of the electronic transitions is 2.4 eV. This frequency is close to the frequency of the green line of a 514.5-nm Ar^+ laser. The subsequent measurements were therefore carried out at this line, making it possible to substantially increase the signal-to-noise ratio.

Figure 1 shows a Raman spectrum for a $Pb_{0.93}Sn_{0.07}Se$ sample recorded at $T = 16$ K in $z(z, \frac{x}{y})\bar{z}$ polarization (the exciting light is polarized in x, while the scattered light is not polarized). Two broad peaks are clearly seen at 85 cm^{-1} and 150 cm^{-1}. The nature of the spectrum changes as the temperature is raised to 300 K (Fig. 2) and the intensity decreases with frequency. The sharp spike at 80 cm^{-1} is caused by the defect in one of the channels of the optical multichannel analyzer. Similar spectra were obtained for samples of solid solutions of other compositions.

Let us summarize the elementary excitation which could account for the observed structural features of the Raman spectrum. Such excitations basically are phonons, whose frequencies have been determined in neutron measurements.[1,2] For a composi-

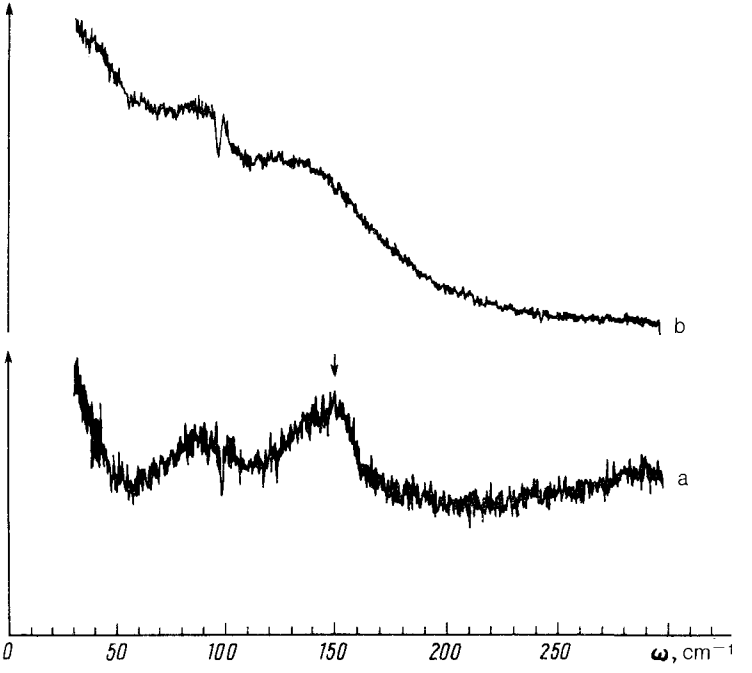

FIG. 1. Raman spectrum of a $Pb_{0.93}Sn_{0.07}Se$ sample, recorded during excitation of the 514.5-nm lines of AR^+ laser in the $z(x, y)z$ polarization. (a) $T = 16$ K; (b) $T = 300$ K.

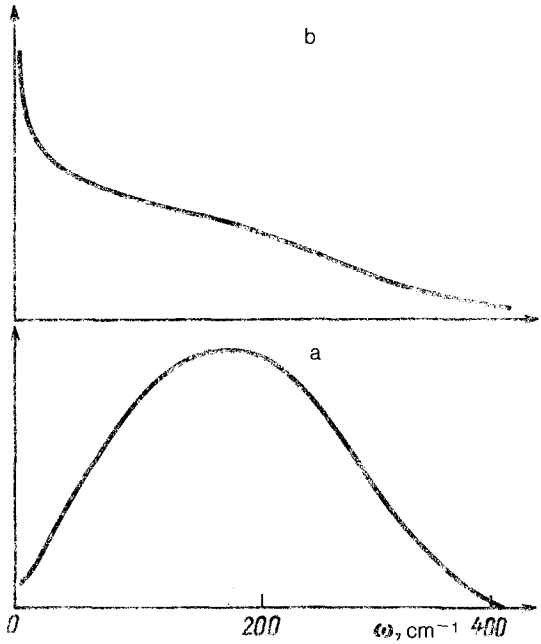

FIG. 2. Raman scattering intensity, calculated from Eq. (4), for $n = 5.3$ and $\kappa = 2$. (a) $T = 16$ K; (b) $T = 300$ K.

tion with $x = 0.07$ the frequencies are $\omega_{TO} = 44\ \text{cm}^{-1}$ and $\omega_{LO} = 140\ \text{cm}^{-1}$. They do not correspond to the Raman scattering peaks and are not seen here, which is attributable to the selection rules for a crystal with an inversion center.

Let us consider plasmons or polaritons whose frequencies are determined by the dispersion relation

$$\left(\frac{cq}{\omega}\right)^2 = \epsilon_\infty + \frac{\omega_0^2}{\omega_0^2 - \omega^2}(\epsilon_0 - \epsilon_\infty) - \frac{\omega_n^2}{\omega^2}. \tag{1}$$

The first two terms on the right side of (1) describe the effect of the polar lattice on the dielectric constant and the last term is the effect of the carriers with a plasma frequency $\omega_n = (4\pi Ne^2/m)^{1/2}$. The values $\epsilon_0 = 300$ and $\epsilon_\infty = 28$ correspond to the values of ω_{LO} and ω_{TO} given above ($\omega_{LO} = \omega_0\sqrt{\epsilon_0/\epsilon_\infty}$, $\omega_{TO} = \omega_0$). In a sample with $x = 0.07$ the carriers are the electrons with an effective mass $m = 0.07 \times 10^{-27}$ g, density $N = 3\times10^{18}\ \text{cm}^{-3}$, plasma frequency $\omega_n = 1.9\times10^3\ \text{cm}^{-1}$, Fermi momentum $k_F = 2.8\times10^6\ \text{cm}^{-1}$, and Fermi velocity $v_F = 4\times10^7$ cm/s. As can be seen from Eq. (1), the polariton spectrum consists of two regions $0 < \omega < \omega_0$ and $\omega > \omega_n/\sqrt{\epsilon_\infty} = 360\ \text{cm}^{-1}$; in determining the boundaries of the region we applied the condition $\omega_n^2 \gg \epsilon_0\omega_0^2$, which is satisfied in our case. There are thus no polaritons in the frequency interval of interest to us.

Let us now consider the electronic excitations. The properties of these excitations depend strongly on the relationship between the mean free path of the carriers, l, and the distance $\lambda \sim 10^{-5}$ cm, over which the electromagnetic field in the sample varies.

When the value of l is small ($l \ll \lambda$), the Raman scattering occurs on the diffusions[6] and when the value of l is large, it occurs on the electron–hole pairs.[5] The value of l is determined from the mobility which reaches values as high as $\mu \sim 5 \times 10^4$ cm^2/(V·s) at low temperatures. We thus find $l = \mu \hbar k_F / e$ cm. Accordingly, the excitations are electron–hole pairs which occupy the frequency interval $0 < \omega < v_F q$ if condition $q \ll k_F$ is satisfied. The contribution of these pairs to the density correlator is proportional to the ratio $\omega / v_f q$. To determine the light scattering intensity, we must integrate the density correlator over q with the square matrix element $f = m_{\alpha\beta}^{-1} e_\alpha^{(i)} e_\beta^{(s)}$ averaged over the Fermi surface and with the factor

$$R(q) = \left\{ [q^2 - (n^2 - \kappa^2)(2\frac{\omega^{(i)}}{c})^2]^2 + 2^6 n^2 \kappa^2 \left(\frac{\omega^{(s)}}{c} \right)^4 \right\}^{-1}, \qquad (2)$$

which takes into account the distribution of the electric field in the sample. The direction of the electric field in the incident and scattered light is set by the vectors $\bar{e}^{(i)}$ and $\bar{e}^{(s)}$ and the effective mass depends on the corresponding frequencies.

$$m_{\alpha\beta}^{-1} = m_0^{-1} \delta_{\alpha\beta} + \frac{1}{m_0^2} \sum_v \left(\frac{p_{cv}^\alpha p_{vc}^\beta}{\epsilon_F - \epsilon_v(k) + \omega^{(i)}} + \frac{p_{cv}^\beta p_{vc}^\alpha}{\epsilon_F - \epsilon_v(k) - \omega^{(s)}} \right), \qquad (3)$$

where the subscript v specifies the energy bands, the transition to which accounts for the resonance intensification.

The ordinary effective mass at the bottom of the conduction band is given by expression (3) with $k = 0$ and $\omega^{(i)} = \omega^{(s)} = 0$, while the principal contribution to it comes from the nearest zone v, for which the denominator in (3) is too small. This remark involves the Debye screening of the density fluctuations. For the relevant carrier concentration the Debye radius $r_D = 10^{-6}$cm is small in comparison with the characteristic value of λ ($\lambda \sim q^{-1}$) determined in the integration of expression (2), in which n and κ are the refractive index and the attenuation factor at the frequency of the incident light, $\omega^{(i)} \approx \omega^{(s)}$. With $\kappa \ll n$, the characteristic value of q coincides with twice the wave vector of light in the medium, which corresponds to the inverse scattering geometry. The Debye screening arises when the Coulomb interaction of the carriers is taken into account. For low transmitted frequencies and small wave vectors the value of the matrix element f averaged over the Fermi surface is subtracted in this case from the matrix element.[7] This means that in the case of Debye screening Raman scattering can be observed only if the matrix element is anisotropic. Resonance intensification is particularly strong if the effective mass at the bottom of the band is isotropic. In this case the polarization dependence has a distinctive nature: In contrast with the isotropic case, the scattering is observed even in the crossed polarizations of the incident and scattered light.

The intensity of the scattered light is proportional to

$$I = \frac{\omega}{1 - e^{\frac{-\hbar\omega}{k_0 T}}} \int_{\omega/v_F}^{\infty} R(q) \frac{dq}{q} \sim \frac{\omega}{1 - e^{\frac{-\hbar\omega}{k_0 T}}} \left\{ \ln \left[\left(1 + \frac{x^2 + y^2}{z^2} \right)^2 - \left(2\frac{x}{z} \right)^2 \right] + \frac{x^2 - y^2}{xy} \left(\tan^{-1} \mathrm{h} \frac{z + x}{y} - \tan^{-1} \mathrm{g} \frac{z - x}{y} \right) \right\} \qquad (4)$$

where

$$z = \omega/v_F, \quad \omega = \omega^{(s)} - \omega^{(e)}, \quad x + iy = 2\frac{\omega^{(e)}}{c}[n^2 - \kappa^2 + 2in\kappa]^{1/2}.$$

The refractive index for $\lambda = 514.5$ nm is $n = 5.3$ and the attenuation factor under conditions of resonance absorption has not been measured. We have plotted the curve of (4) for several values of κ. The curve has only one peak which is displaced toward lower frequencies as κ is increased. The peak also changes its shape: it becomes more symmetric as κ is increased. The parameter $\kappa = 2$, for which the curves in Fig. 2 were plotted for two temperatures, corresponds most closely to the spectrum observed at $T = 16$ K. The shape and position of the peak are in fair agreement with the result obtained experimentally at $\omega = 150$ cm^{-1}. We have no plausible explanation of the second experimentally observed peak at $\omega \approx 85$ cm^{-1}.

[1]L. K. Vodopyanov, I. V. Kucherenko, A. P. Shotov, and R. Scherm, *Proceedings of the International Conf. on Lattice Dynamics*, Paris, 1978, p. 673.
[2]L. K. Vodop'yanov, I. K. Kucherenko, A. P. Shotov, and R. Sherm, Pis'ma Zh. Eksp. Teor. Fiz. **27**, 101 (1978) [JETP Lett. **27**, 92 (1978)].
[3]S. Prakash, H. Gupta, and B. Tripathi, J. Chem. Phys. **7**, 663 (1983).
[4]P. Lin and L. Kleiman, Phys. Rev. **142**, 478 (1966).
[5]A. A. Abrikosov and L. A. Fal'kovskiĭ, Zh. Eksp. Teor. Fiz. **40**, 262 (1961) [Sov. Phys. JETP **13**, 179 (1961)].
[6]L. A. Fal'kovskiĭ, Zh. Eksp. Teor. Fiz. **95**, 1145 (1989) [Sov. Phys. JETP **68**, 661 (1989)].
[7]A. A. Abrikosov and V. M. Genkin, Zh. Eksp. Teor. Fiz. **65**, 842 (1973) [Sov. Phys. JETP **38**, 417 (1974)].

Translated by S. J. Amoretty